Ocean Engineering 168 (2018) 95–107

Contents lists available at ScienceDirect

Ocean Engineering

journal homepage: www.elsevier.com/locate/oceaneng

Stability analysis of a composite breakwater at Yantai port, China: An application of FSSI-CAS-2D

Kunpeng He[a,c], Taikun Huang[b], Jianhong Ye[a,*]

[a] State Key Laboratory of Geomechanics and Geotechnical Engineering, Institute of Rock and Soil Mechanics, Chinese Academy of Sciences, Wuhan, 430071, China
[b] CCCC First Harbour Consultants CO. LTD, Tianjin, 300222, China
[c] University of Chinese Academy of Sciences, Beijing, 100049, China

ARTICLE INFO

Keywords:
Composite breakwater
Stability analysis
FSSI-CAS-2D
Liquefaction
West harbour zone
Yantai port

ABSTRACT

In offshore areas, quaternary loose seabed soils widely distribute around the world, and a great number of offshore structures actually have been constructed on quaternary seabed floors. In practical engineering, it is highly necessary to evaluate the stability of offshore structures built on quaternary seabed floors under the impact of extreme ocean waves. Based on the VARANS equation and the dynamic Biot's equation, an integrated numerical model FSSI-CAS 2D has been developed by Ye et al. (2013b) to investigate the interaction between ocean waves, marine structures and their seabed foundations. In this study, taking the composite breakwater project in the west harbour zone of Yantai port in China as an engineering case, the integrated numerical model FSSI-CAS-2D is used to evaluate the stability of the composite breakwater under the impact of fortified ocean waves with a 50 years recurrence period. Computational results indicate that the composite breakwater at west harbour zone of Yantai port would be generally stable during its service life. This application demonstrates that the integrated model FSSI-CAS-2D is applicable, and suitable for practical engineering. The case study illustrated in this study can provide ocean engineers with an excellent case demonstration of engineering application, to evaluate the stability of offshore structures under the impact of extreme ocean waves.

1. Introduction

In last 20 years, a great number of marine structures, such as breakwaters, have been constructed in offshore areas. The stability of offshore marine structures under ocean wave loading is the main concern of ocean engineers involved in design. In offshore environment, newly deposited Quaternary seabed soil is widely distributed, for example, the loose silty soil in the zone of the estuary of Yellow River in China. Actually, a great number of offshore structures have been built on Quaternary sediments. The particle arrangement of Quaternary seabed soil generally is relatively loose, far from being very dense. Under cyclic ocean wave loading, seabed soil particles re-arrange their relative positions to a more dense status, accompanied by a pore water drainage process. In this process, the pore water pressure builds up, making soil liquefy, or soften. As a result, the overlaying marine structures would lose their stability. Therefore, it is of great importance to quantitatively evaluate the stability of offshore marine structures constructed on quaternary loose seabed floors.

The preconditions for evaluating the stability of offshore marine structures include two aspects: (1) understanding the mechanism of wave-structure-seabed interaction, (2) development of numerical models for stability evaluation. In early stage, analytical solutions were widely proposed to study the mechanism of wave-seabed interaction, in which marine structures could not be considered. Due to the limitation of analytical methods, seabed soil must be very dense in which elastic deformation is dominant under wave loading. In analytical solutions, the dense seabed could be infinite (Yamamoto et al., 1978; Madsen, 1978) or finite (Hsu and Jeng, 1994; Jeng and Hsu, 1996) in depth; it also could be isotropic or anisotropic. The waves adopted in these analytical solutions were all based on Stokes wave theory, involving progressive wave, standing wave or short-crested wave (Hsu and Jeng, 1994). The governing equation for seabed soil could be the consolidation equation, the 'u-p' approximation, and the 'u-w' equation (Liao et al., 2015). Actually, the uncoupled method was adopted in these analytical solutions. There was no feedback from seabed soil to ocean wave when seabed responding to ocean wave. Besides, numerical methods are also powerful tool to investigate the wave-seabed interaction. However, most previous numerical investigations were also limited to very dense elastic seabed soil, such as those in Ye and Jeng (2012), Gatmiri (1990), Jeng and Lin (1996), Zhou et al. (2005) and

* Corresponding author.
E-mail address: yejianhongcas@gmail.com (J. Ye).

https://doi.org/10.1016/j.oceaneng.2018.09.004
Received 14 February 2018; Received in revised form 23 July 2018; Accepted 1 September 2018
Available online 11 September 2018
0029-8018/

Luan and Wang (2001). For the interaction between ocean waves and loose seabed floors, few investigations were undertaken. Until recently, Yang and Ye (2017) and Yang and Ye (2018) systematically study the dynamics characteristics of loose seabed floor under the impact of standing wave, and wave-current.

For the scientific problem of wave-structure-seabed interaction, it seems that numerical methods are the only feasible ways, due to the complexity of the interaction between ocean wave, marine structures and their seabed foundations. Mase et al. (1994) developed a FEM numerical model to investigate the wave-induced pore water pressures and effective stresses in a sandy seabed foundation beneath a composite caisson-type breakwater based on Biot's consolidation equation. After that, Mizutani et al. (1998) and Mizutani et al. (1999) developed a BEM-FEM combination numerical model to study the wave-seabed-structure interaction by adopting a prototype model. Their work greatly promoted the progress on wave-structure-seabed interaction. However, the numerical models proposed by Mase et al. (1994) and Mizutani et al. (1998) could not yet be applied in practice engineering due to the following two reasons. First, the potential flow theory involving Laplace's equation used in Mizutani et al. (1998) could not simulate the complicated motion of seawater in extreme ocean waves, such as breaking and turbulence, in real-life large scale cases. Second, only a poro-elastic soil model could be used in their numerical models. As presented above, a great number of offshore structures have been built on Quaternary loose seabed floor. The wave-induced behaviour of loose seabed foundation must be characterized using poro-elasto-plastic soil models.

To overcome the above two difficulties, Ye et al. (2013b) developed an integrated model FSSI-CAS 2D for the problem of fluid-structures-seabed interaction (FSSI). In the integrated model FSSI-CAS 2D, the Volume Average Renolds Average Navier Stokes (VARANS) equation was adopted to simulate the complicated motion of seawater in ocean waves, as well as porous flow in porous seabeds; the dynamic Biot's equation was adopted to describe the nonlinear behaviour of marine structures and their seabed foundations. A one-way integrating algorithm, based on the radial point interpolation method, was developed to link the two equations by guaranteeing the continuity of pressure and velocity at interfaces between the seawater domain and the seabed foundation, marine structures. The integrated model FSSI-CAS 2D has been widely validated by an analytical solution and a series of wave flume tests (Ye et al., 2013b). Most importantly, several poro-elasto-plastic soil models, such as Mohr-Coulomb, Modified Cambridge Clay, Pastor-Zienkiewics-Mark III etc., are available to describe the behaviour of loose seabed foundation in FSSI-CAS 2D. So far, this integrated numerical model has been successfully applied to investigate the dynamics of composite breakwater and its seabed foundation involving breaking wave (Ye et al., 2014), tsunami wave (Ye et al., 2013a) and loose seabed soil (Ye et al., 2015). It is indicated by these successful cases that the integrated model FSSI-CAS 2D can be applied in practice engineering to evaluate the stability of offshore marine structures.

In this study, taking the composite breakwater project at the west harbour zone of Yantai port in China as the engineering case, the integrated numerical model FSSI-CAS-2D was adopted to evaluate the stability of the composite breakwater under the impact of fortified ocean waves with a 50 years recurrence period. Computational results indicate that the composite breakwater at west harbour zone of Yantai port would be generally stable in its service life. This case application demonstrates that the integrated model FSSI-CAS-2D is applicable in the practical engineering; and this integrated model also can be utilized to optimize the design of offshore structures in the future.

2. Integrated model FSSI-CAS 2D

2.1. Governing equations

The dynamic Biot's equation, known as "$u-p$" approximation proposed in Zienkiewicz et al. (1980), is used to describe the dynamic response of porous medium under earthquake loading. In this formulation, the relative displacements of pore fluid to soil particles are ignored, but the acceleration of the pore water and soil particles are included:

$$\frac{\partial \sigma_x'}{\partial x}+\frac{\partial \tau_{xz}}{\partial z}=-\frac{\partial p_s}{\partial x}+\rho\frac{\partial^2 u_s}{\partial t^2}, \tag{1}$$

$$\frac{\partial \tau_{xz}}{\partial x}+\frac{\partial \frac{\partial \sigma_z'}{\partial x}+\frac{\partial \tau_{xz}}{\partial z}=-\frac{\partial p_s}{\partial x}+\rho\frac{\partial^2 u_s}{\partial t^2}}{\partial z}+\rho g=-\frac{\partial p_s}{\partial z}+\rho\frac{\partial^2 w_s}{\partial t^2}, \tag{2}$$

$$k\nabla^2 p_s-\gamma_w n\beta\frac{\partial p_s}{\partial t}+k\rho_f\frac{\partial^2 \varepsilon_v}{\partial t^2}=\gamma_w\frac{\partial \varepsilon_v}{\partial t}, \tag{3}$$

where (u_s, w_s) are displacements of the soil in horizontal and vertical directions, respectively; n is soil porosity; σ_x' and σ_z' are effective normal stresses in the horizontal and vertical directions, respectively; τ_{xz} is shear stress; p_s is the pore water pressure; $\rho=\rho_f n+\rho_s(1-n)$ is the average density of porous seabed; ρ_f is the fluid density; ρ_s is solid density; k is the Darcy's permeability; g is the gravitational acceleration; γ_ω is specific weight of water and ε_v is the volumetric strain. In equation (3), the compressibility of pore fluid (β) and the volume strain (ε_v) are defined as

$$\beta=\left(\frac{1}{K_f}+\frac{1-S_r}{p_{w0}}\right),\quad \text{and}\quad \varepsilon_v=\frac{\partial u_s}{\partial x}+\frac{\partial w_s}{\partial z}, \tag{4}$$

where S_r is the degree of saturation of seabed, p_{w0} is the absolute static pressure and K_f is the bulk modulus of pore water. In general, $K_f=2.24\times10^6$ kPa.

The finite element method is used to solve the above governing equations (1)–(3). The discretized governing equations are

$$\mathrm{M}\ddot{\mathbf{u}}+\mathrm{K}\mathbf{u}-\mathrm{Q}\mathbf{p}=f^{(1)} \tag{5}$$

$$\mathrm{G}\ddot{\mathbf{u}}+\mathrm{Q}^{\mathrm{T}}\dot{\mathbf{u}}+\mathrm{S}\dot{\mathbf{p}}+\mathrm{H}\mathbf{p}=f^{(2)} \tag{6}$$

The Generalized Newmark p^{th} order scheme for j^{th} order equation is adopted as the numerical integration when solving the above discretized equations. The definition of the coefficient matrices M, K, Q, G, S, H, $f^{(1)}$, , and the detailed information for the numerical method to solve the Biot's equation can be found in Ye (2012); Ye et al. (2013b); Zienkiewicz et al. (1999).

For the problem of Fluid-Structure-Seabed Interaction (FSSI), a coupled numerical model FSSI-CAS 2D was developed by Ye (2012). In FSSI-CAS 2D, the Volume Average Reynolds Average Navier Stokes (VARANS) equation (Hsu et al., 2002) governs wave motion and porous flow in porous seabed. The above dynamic Biot's equation governs the dynamic behaviour of offshore structure and its seabed foundation. A coupled algorithm is developed to couple the VARANS equation and Biot's dynamics equation together. More detailed information about the coupled model can be found in Ye et al. (2013b), Ye (2012) and Zienkiewicz et al. (1999).

In this study, large deformation occurs in the seabed foundation near to breakwater built on loose liquefiable seabed under seismic wave shaking. The updated Lagrangian method is adopted to deal with this large deformation problem. In the computation, the coordinates of nodes, status variables of soil, which are dependent on the effective stress history, such as void ratio e and permeability k are updated in each time step based on deformation. Correspondingly, the coefficient matrices M, K, Q, G, S, H, $f^{(1)}$, , as well as boundary values on boundaries are also updated.

2.2. Constitutive model: Pastor-Zienkiewics-Mark III

Based on classical plasticity theory, the constitutive relationship for the effective stress and strain of the soil can be written as:

$$\sigma_{ij}'=\mathrm{D}_{ijkl}^{ep}\varepsilon_{kl} \tag{7}$$

Fig. 1. Position of Yantai port locating at (E121.3537, N37.6183).

where ε_{kl} is the strain of soil, D^{ep}_{ijkl} is the elasto-plastic modulus:

$$D^{ep}_{ijkl} = D^{e}_{ijkl} - \frac{D^{e}_{ijmn} m_{mn} n_{st} D^{e}_{stkl}}{H_{L/U} + n_{st} D^{e}_{stkl} m_{kl}} \tag{8}$$

where $D^{e}_{ijkl} = 2G\left(\delta_{ik}\delta_{jl} + \frac{\nu}{1-2\nu}\delta_{ij}\delta_{kl}\right)$, G and ν are the elastic shear modulus and Poisson's ratio, respectively. $H_{L/U}$ is the plastic modulus at loading or unloading stage. m_{mn} is a unit tensor for the plastic flow direction, n_{st} is the unit tensor for loading or unloading direction. The above directional tensors are formulated as:

$$m_{mn} = \frac{\left(\frac{\partial g}{\partial \sigma'_{mn}}\right)}{\left\|\frac{\partial g}{\partial \sigma'_{mn}}\right\|} \text{and } n_{st} = \frac{\left(\frac{\partial f}{\partial \sigma'_{st}}\right)}{\left\|\frac{\partial f}{\partial \sigma'_{st}}\right\|} \tag{9}$$

where $\|\cdot\|$ represents tensor norm, f and g are the yield function and plastic potential function in stress space. An associated flow rule is implied if $f = g$. Otherwise, a non-associated flow rule is applied.

In this study, the elasto-plastic constitutive model PZIII, proposed by Pastor et al. (1990) based on the generalized plastic theory, is adopted to describe the dynamic behaviour of loose seabed foundation under seismic wave. In PZIII, the yield surface function f and plastic potential surface function g are defined as

$$f = q' - M_f p'\left(1 + \frac{1}{\alpha_f}\right)\left[1 - \left(\frac{p'}{p'_f}\right)^{\alpha_f}\right] = 0 \tag{10}$$

$$g = q' - M_g p'\left(1 + \frac{1}{\alpha_g}\right)\left[1 - \left(\frac{p'}{p'_g}\right)^{\alpha_g}\right] = 0 \tag{11}$$

The plastic modulus at loading and unloading stage are defined as:

$$H_L = H_0 p'\left(1 - \frac{q'/p'}{\eta_f}\right)^4 \left[1 - \frac{q'/p'}{M_g} + \beta_0\beta_1 exp(-\beta_0\xi)\right]\left(\frac{q/p'}{\eta_{max}}\right)^{-\gamma_{DM}} \tag{12}$$

$$H_U = \begin{cases} H_{u0}\left(\frac{M_g}{\eta_u}\right)^{\gamma_U} & \text{for} \left|\frac{M_g}{\eta_u}\right| > 1 \\ H_{u0} & \text{for} \left|\frac{M_g}{\eta_u}\right| \le 1 \end{cases} \tag{13}$$

where the p' and q' is the mean effective stress and deviatoric stress, respectively. $\eta_f = \left(1 + \frac{1}{\alpha_f}\right)M_f$, η_{max} is the maximum stress ratio ($\frac{p'}{q'}$), and η_u is the stress ratio at the unloading point. M_f, M_g, α_f, α_g, β_0, β_1, γ and γ_{DM} are the parameters describing the properties of sandy soil. The detailed information about the PZIII model can be found in Pastor et al. (1990) and Zienkiewicz et al. (1999). PZIII is an excellent constitutive model for describing the behaviour of clay and sandy soil. Its reliability has been validated by a series of laboratory tests under monotonic and cyclic loading (Zienkiewicz et al., 1999).

2.3. Verification

The validity and reliability of the developed integrated numerical model FSSI-CAS 2D have been widely verified by Ye (2012). Adopting the analytical solution proposed by Hsu and Jeng (1994), and a series of laboratory wave flume tests conducted by Lu (2005) for regular wave and cnoidal wave, Tsai and Lee (1995) for standing wave, Mizutani et al. (1998) for submerged breakwater, and Mostafa et al. (1999) for composite breakwater, the developed semi-coupled numerical model FSSI-CAS 2D was used to reproduce the dynamic response of elastic seabed foundation and/or breakwater. The good agreement between the predicted numerical results and the corresponding experimental data indicated that FSSI-CAS 2D is a highly reliable for the problem of Wave-seabed-Structure Interaction. Furthermore, the validity and reliability of FSSI-CAS 2D for the problem of wave-loose seabed soil interaction was also verified by a wave flume test (Teh et al., 2003) and a geotechnical centrifuge test (Sassa and Sekiguchi, 1999). More detailed information about the verification work can be found in Ye (2012); and related work has been published in (Ye et al., 2013b). Additionally, the integrated model FSSI-CAS 2D, incorporating PZIII soil model has been successfully applied to investigate the dynamics and stability of an idealized composite breakwater built on a loose seabed foundation (Ye et al., 2015).

3. Engineering background

Yantai port is located on the southwest coastal line of Bohai Bay, China. It is geographically affiliated to the city of Yantai, Shandong Province, China, as illustrated in Fig. 1. Currently, Yantai port includes four harbour zones. They are chifu bay zone, west harbour zone, longkou harbour zone and penglai harbour zone, respectively. Among them, the west harbour zone is the largest one; and is a core asset for development of the Yantai port. Total length of the wharfs in the west harbour zone is 19 km. The maximum water depth in front of the wharfs is 28 m. The west harbour zone is divided into 8 functional zones such as container, chemical liquid, bulk cargo, general bulk, crude oil and LNG etc. Totally, 65 berths with capacity 50,000 to 300,000 tons will be constructed. The planned ultimate bearing capacities of the west harbour zone will be up to 200 million tonnes and 15 million standard containers per year.

In order to guarantee the safety of vessels when docking in front of

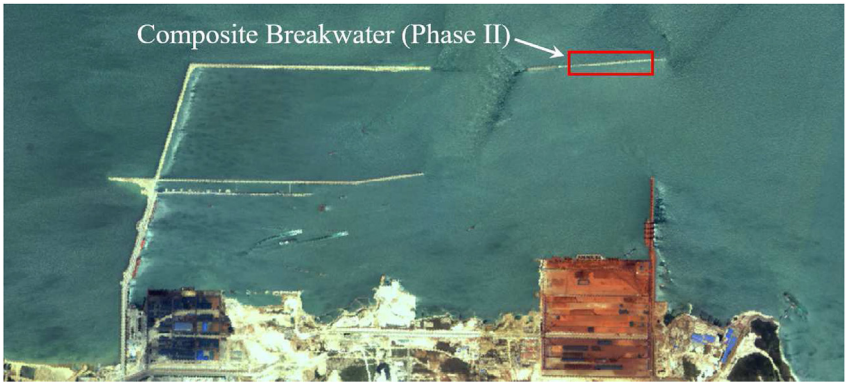

Fig. 2. Satellite top view of the west harbour zone of Yantai port.

the wharfs for loading and unloading, a group of deep water breakwaters have been constructed to surround a harbour basin with area about 5 km^2, as illustrated in Fig. 2. In the west harbour zone, the whole breakwater construction project is divided into two phases. The structure form of phase I is the sloping rubble mound breakwater covered by accropodes; and it is the composite breakwater in phase II, as shown in Fig. 3. Currently, the construction of breakwaters in phase I and phase II have all been finished. Undoubtedly, the stability of these breakwaters under extreme ocean waves is the key factor for the long-term service ability of west harbour zone of Yantai port. It is of great significance to evaluate the stability of the breakwaters at the west harbour zone of Yantai port.

In this study, taking the composite breakwaters in phase II of the west harbour zone as the representative, the newly developed model FSSI-CAS 2D is adopted to evaluate the stability of the composite breakwaters under fortified ocean wave. To implement this application, the profiles and basic physical properties of the seabed soil layers, which is as the foundation of the breakwaters at the west harbour zone, were collected from the company in charge of the in-situ geotechnical survey for the phase II project. As demonstrated in Fig. 4, there are mainly five soil layers in the seabed foundation of the breakwaters. They are muddy-silt clay ①$_1$, Silty Clay ①$_2$, Clay ③$_1$, Silty Clay ③$_2$ and Silt ③$_4$, respectively. Their basic physical properties of the five seabed soil layers obtained by performing a series of geotechnical tests are listed in Table 1. It can be seen that the muddy-silt clay ①$_1$ and ①$_2$ are the weak soil layers with thickness of 12 m–14 m. Their water content is up to 39.6% and 32.3%; void ratio is around 1.0; and the bearing capacity f is only 70, 90 kPa respectively. In engineering practice, the surface layer of a thickness of 2 m of the first soil layer ①$_1$ exactly beneath the composite breakwater was replaced with coarse sand to enhance the bearing capacity of the seabed foundation. Furthermore, a great number of plastic drainage strips with a length of 12 m were inserted into the soil layers ①$_1$ and ①$_2$ with a spacing of 1.0 m, to improve

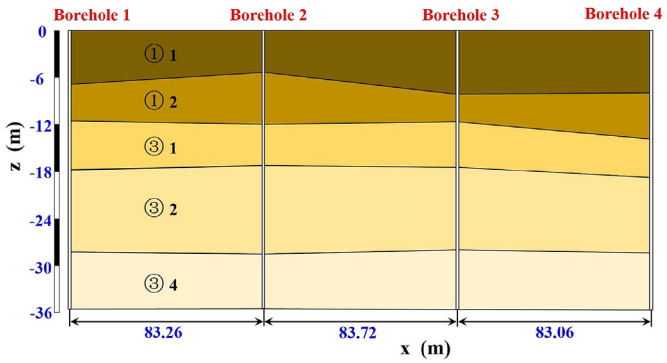

Fig. 4. Profiles of seabed foundation soil layers coming from field boreholes survey. ①$_1$: muddy-silt clay, ①$_2$: Silty Clay, ③$_1$: Clay, ③$_2$: Silty Clay and ③$_4$: Silt.

their seepage permeability. This engineering measure can effectively to accelerate the process of consolidation of the seabed foundation, as well as the subsiding of overlying composite breakwaters. In Table 1, it is also can be found that the seabed soil layers ③$_1$, ③$_2$, ③$_3$ all have excellent bearing performance with bearing capacities are in the range of 180 kPa–200 kPa.

Fortified parameters of ocean wave for the breakwaters in the west harbour zone of Yantai port also are necessary in design practice for the evaluation of stability of these breakwaters. A third party consulting company was employed by the owner of Yantai port to specially observe the ocean wave parameters in the area near to the west harbour zone in long term. Based on the long term observation data of ocean waves, the owner of Yantai port set out the fortified parameters of ocean wave for the breakwaters in the west harbour zone, as listed in Table 2, in which $H_{1\%}$ is the average height of the highest 1% wave height, $H_{5\%}$ is the average height of the highest 5% wave height, and $H_{13\%}$ is the average height of the highest 13% wave height.

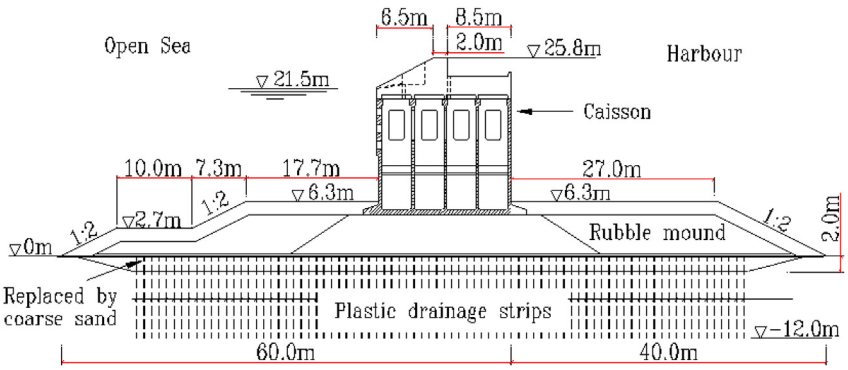

Fig. 3. Section and dimensions of the composite breakwater at Yantai port.

Table 1
Basic physical properties of seabed foundation soil layers.

Stratum	w	γ	e	W_L	I_p	I_L	ϕ'	c'
	(%)	(kN/m^3)		(%)	(%)		(°)	(kPa)
Muddy-silty Clay ①$_1$	39.6	17.9	1.08	32.1	14.5	1.52	18.1	15
Silty Clay ①$_2$	32.3	18.5	0.91	29.3	13.1	1.24	19.9	20
Clay ③$_1$	27.5	19.5	0.77	42.8	21.3	0.28	23.4	35
Silty Clay ③$_2$	23.4	20.0	0.64	28.2	12.8	0.63	27.1	26
Silt ③$_4$	22.3	19.9	0.62	24.7	7.4	0.66	25.5	38

Stratum	$a_{v0.1-0.2}$ (MPa)	$E_{s0.1-0.2}$ (MPa)	C_C	SPT (N)	f (kPa)	k (m/s)	C_{vV} (cm^2/s)	C_{vH} (cm^2/s)
Muddy-silty Clay ①$_1$	0.73	2.92	0.26	1.0	70	3.7×10^{-7}	1.72×10^{-3}	2.35×10^{-3}
Silty Clay ①$_2$	0.52	3.94	0.21	2.0	90	2.6×10^{-7}	4.12×10^{-3}	4.80×10^{-3}
Clay ③$_1$	0.28	6.66	0.23	15.0	180	9.6×10^{-6}	1.00×10^{-3}	0.95×10^{-3}
Silty Clay ③$_2$	0.26	6.76	0.15	13.0	180	4.0×10^{-6}	4.33×10^{-3}	4.05×10^{-3}
Silt ③$_4$	0.18	9.42	0.11	28.0	200	5.8×10^{-6}	8.54×10^{-3}	8.13×10^{-3}

Table 2
Fortified parameters of ocean wave for the breakwaters in west harbour zone.

Recurrence period	Water level (m)	$H_{1\%}$ (m)	$H_{5\%}$ (m)	$H_{13\%}$ (m)	Mean period T (s)
50 years	Extreme high level +3.56	6.5	5.4	4.6	9.6
	Design high level +2.46	6.4	5.3	4.5	
	Design low level +0.25	6.2	4.5	4.4	
10 years	Extreme high level +3.56	5.4	4.5	3.8	8.3
	Design high level +2.46	5.3	4.4	3.7	
	Design low level +0.25	5.1	4.3	3.6	

In this study, in order to examine the stability of the composite breakwater in the west harbour zone under the most extreme sea state, the ocean wave parameters related to the 50 years recurrence period are chosen. They are 6.5 m in wave height, 9.6s in wave period and +3.56 m in water level elevation. Due to the fact that the average elevation of the seabed foundation surface is −18 m, the water depth in this study is 21.5 m.

4. Computational domain, boundary condition and soil parameters

According to the design diagram of the composite breakwater in the west harbour zone of Yantai port, shown in Fig. 3, and the profiles of seabed soil layers in Fig. 4, the computational domain used in this study to evaluate the stability of the composite breakwater of phase II project in the west harbour zone of Yantai port is illustrated in Fig. 5. The total length of the computational domain is 750 m (x = 350 m to x = 1100 m). The width of the rubble mound is 100 m. Its distance to the left and right boundary of the seabed foundation is 400 m and 250 m, respectively. Due to the fact the maximum depth of surveying boreholes in the seabed floor on which this composite breakwater is built is only 35.5 m, the thickness of the seabed foundation in the computation is set as 35.5 m, correspondingly. In this study, the seabed surface is set as z = 0 m; and the left side of the seabed foundation is set as x = 350 m. The wave maker is located at x = 0 m in the fluid domain. The distance from the wave maker to the composite breakwater is 750 m, about 6 times of the wave length.

In stability analysis, the following boundary conditions are applied.

(1) The lateral sides of seabed foundation are fixed in horizontal.

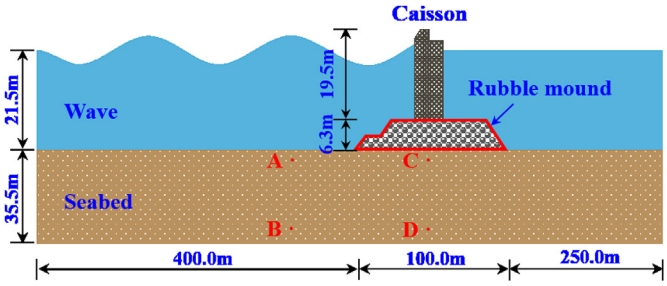

Fig. 5. Computational domain and dimensions of breakwater at west harbour zone of Yantai port.

$$u_s|_{left\ side} = u_s|_{right\ side} = 0 \tag{14}$$

(2) The bottom of seabed foundation is fixed in both horizontal and vertical, and treated as a impermeable board.

$$u_s = w_s = 0 \quad and \quad \frac{\partial p_s}{\partial z} = 0 \quad at \quad z = -35.5m \tag{15}$$

(3) On the surface of the seabed floor and the outer surfaces of the composite breakwater, the total pressure including hydrostatic and wave-induced hydrodynamic pressure is applied.
(4) Since the caisson is made of concrete, it can be treated as an impermeable object. As a result, an upward buoyancy acting on the bottom of the caisson induced by hydrostatic and wave-induced hydrodynamic pressure must be applied.

It is an indisputable fact in the field of geomechanics that the reliability of the computational results is highly dependent on the accuracy of soil/rock's physical parameters. In this study, the constitutive soil model PZIII is used to describe the mechanical behaviour of the seabed soil foundation. Therefore, it is necessary to determine the model parameters needed by PZIII model for the five soil layers of the seabed foundation. However, only conventional geotechnical testing work in the field survey stage was conducted according to the Code for Investigation of Geotechnical Engineering of Ports (JTS 133-1-2010), and the Code of Design and Construction of Breakwaters (JTS 154-1-2011) in China. At the design stage, it was not planned that the integrated model FSSI-CAS 2D would be applied to examine the stability of the composite breakwater in the west harbour zone of Yantai port. As a result, geotechnical testing work, such as dynamic triaxial test, to determine the model parameters of the five layers seabed foundation soil for PZIII soil model was not performed. The only way is to estimate these model parameters of the seabed foundation soil based on their

basic properties, as listed in Table 1. In the future, a series of geotechnical tests are highly recommended to be conducted to determine the model parameters of seabed foundation soil if FSSI-CAS 2D is adopted to examine the stability of offshore structures.

In the PZIII soil model, there are totally 13 soil parameters. Among them, p_0' is a reference pressure at which the soil parameters measured in the tests. As listed in Table 1, the deformation modulus of soil E_S was measured in the stress range of 100–200 kPa. Based on this, p_0' is estimated as 150 kPa in this study. K_{evo} and G_{eso} is the bulk modulus and shear modulus of soil at reference pressure p_0', respectively, estimated according to the following theoretic formulations:

$$E = \frac{(1+\nu)(1-2\nu)}{(1-\nu)}E_s \tag{16}$$

$$K_{evo} = \frac{E}{3(1-2\nu)} \quad and \quad G_{eso} = \frac{E}{2(1+\nu)} \tag{17}$$

where ν is Poisson's ratio of soil. According to previous experience, $\nu = 0.38$ for soil layers ①$_1$ and ①$_2$; $\nu = 0.3$ for soil layers ③$_1$, ③$_2$ and ③$_3$. M_f is the slope of critical state line (CSL) of soils, one can be estimated as

$$M_f = \frac{6\sin(\phi)}{3-\sin(\phi)} \tag{18}$$

in which ϕ is the friction angle of soil. M_g is a soil parameter related to plastic potential surface, similar to M_f. Generally, M_g is less than M_f. In this study, M_g/M_f is set as 0.9 referring to the soil parameters of Nevada sands given by Zienkiewicz et al. (1999). H_0 is a parameter describing the modulus of soil at the first loading stage (elastic deformation is dominant). Referring the elastic modulus E at p_0', H_0 can be estimated as $H_0 = E/p_0'$ according to the definition of loading modulus H_L in Equation (12). H_{U0} is the unloading modulus of soil at the first unloading stage. If there is no plastic deformation generated at the first unloading stage, then H_{U0} should be equal to the elastic modulus of soil E, in theory. If plastic deformation is generated, H_{U0} should be $E/(1-Ratio_{plastic})$, in which $Ratio_{plastic}$ is the percentage of plastic deformation in the total deformation. Due to the fact that the soil layers ①$_1$ and ①$_2$ are relatively soft and weak, plastic deformation in cyclic loading and unloading processes must be significant. The $Ratio_{plastic}$ is set as 40% for soil layers ①$_1$ and ①$_2$. Meanwhile, the bearing capacity of soil layers ③$_1$, ③$_2$ and ③$_3$ reaches up to around 200 kPa, as illustrated in Table 1, the plastic deformation in cyclic loading and unloading process should be apparently less than that of ①$_1$ and ①$_2$. The $Ratio_{plastic}$ is set as 15% for soil layers ③$_1$, ③$_2$ and ③$_3$ in this study.

The other six parameters α_f, α_g, β_0, β_1, γ_u and γ_{DM} are material coefficients related to soil properties. These material coefficients can be reliably calibrated by geotechnical testing data, such as dynamic triaxial test. Due to the fact that the test data is not available in the current situation, the values suggested by Zienkiewicz et al. (1999) are used in this study. All the estimated soil parameters of the five seabed soil layers for PZIII soil model are listed in Table 3.

The composite breakwater in the west harbour zone of Yantai port consists of concrete caisson and its underlying rubble mound. In stability analysis, the caisson is treated as an impermeable rigid object, and the rubble mound is treated as a kind of porous medium with great porosity. The poro-elastic model is adopted for the caisson and rubble mound, with parameters listed in Table 4. In this study, the saturation of the five soil layers of the seabed foundation soil are all set as 98%. As presented above, a series of plastic drainage strips have been inserted into the soil layers ①$_1$ and ①$_2$ in the zone beneath the composite breakwater to enhance their permeability. To consider this effect, the permeability coefficients of soil layers ①$_1$ and ①$_2$ in the zone beneath the composite breakwater are set to 100 times their original value, as illustrated in Table 1, in the computation.

Table 3
Model parameters of seabed foundation for constitutive model PZIII in analysis.

Parameter	①$_2$	Silty Clay ①$_2$	Clay ③$_1$	Silty Clay ③$_2$	Silt ③$_4$	Unit
E_s	2.92	3.94	6.66	6.67	9.42	[MPa]
ν	0.38	0.38	0.3	0.3	0.3	
E	1.56	2.11	4.95	4.96	7.0	[MPa]
K_{evo}	2167	2931	4125	4133	5833	[kPa]
G_{eso}	565	765	1904	1908	2692	[kPa]
p_0'	150	150	150	150	150	[kPa]
M_g	0.62	0.70	0.83	0.96	0.91	–
M_f	0.69	0.77	0.92	1.07	1.01	–
α_f	0.45	0.45	0.45	0.45	0.45	–
α_g	0.45	0.45	0.45	0.45	0.45	–
β_0	4.2	4.2	4.2	4.2	4.2	–
β_1	0.2	0.2	0.2	0.2	0.2	–
H_0	10.4	14.0	33.0	33.0	46.7	–
H_{U0}	2600	3157	5824	5835	8235	[kPa]
γ_u	2.0	2.0	2.0	2.0	2.0	–
γ_{DM}	4.0	4.0	4.0	4.0	4.0	–

Table 4
Properties of composite breakwater and seabed foundation.

Medium	E (Pa)	ν	k (m/s)	n	S_r
Rubble mound	1.0×10^9	0.33	2.0×10^{-1}	0.4	0.99
Caission	1.0×10^{10}	0.25	1.0×10^{-12}	0.0	0.0

5. Initial condition

In offshore environments, the seabed soil usually experiences consolidation under its own weight. Additionally, seabed foundation beneath breakwaters will be loaded by the weight of breakwater after construction, resulting in the generation of excess pore pressure in seabed foundation at the early stage. Excess pore pressure will be dissipated over time. Meanwhile, breakwater subsides downward, until a new balanced consolidation state is reached. This consolidation process of seabed foundation under a composite breakwater has been studied in Shen et al. (2017). In the stability analysis of the composite breakwater in the west harbour zone, this balanced consolidation state is taken as the initial condition.

In Fig. 6, the distribution of the displacement, effective stresses and pore pressure in the seabed foundation after consolidation is demonstrated. It can be seen that the composite breakwater subsides about 20 cm under its own self-weight after consolidation. Due to the gravity compression of the breakwater, the effective stress σ_z' in the zone under the composite breakwater increases dramatically relative to the zone far away from the breakwater. In the seabed floor away from the composite breakwater, the distribution of effective stress σ_x' and σ_z' is layered, indicating that the effect of offshore structures on effective stress is only limited in the zone around offshore structure itself. It also found that there are two concentration zones of shear-stress in the seabed foundation beneath the composite breakwater due to the gravity compression of breakwater. The maximum magnitude of the shear stress could reach up to about 50 kPa. The distribution of pore pressure in the seabed foundation is layered (hydrostatic pressure), even in the zone beneath the breakwater. It indicates that the excess pore pressure in the seabed foundation has completely dissipated. Due to the impermeability of caisson, the pore pressure in the caisson is all zero.

6. Stability analysis

6.1. Hydrodynamics

Ocean waves are the main driving factor for the failure of offshore

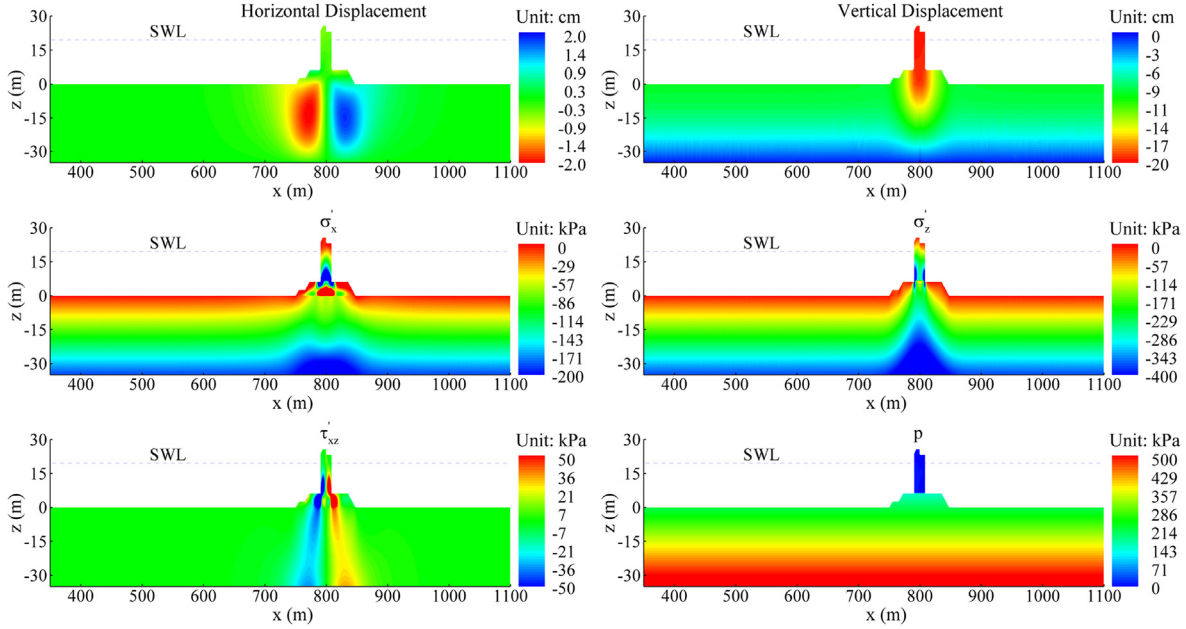

Fig. 6. Distribution of displacements, effective stresses and pore pressure at initial consolidation (T is wave period and T = 9.6 s).

structures in practice. Before examining the stability of the composite breakwater at the west harbour zone of Yantai port under the fortified ocean wave, it is necessary to firstly investigate the characteristics of the fortified ocean wave when it interacts with the composite breakwater and the seabed foundation, so as to determine the wave-induced force acting on the composite breakwater. The wave profile, distribution of pore pressure, dynamic pore pressure, velocity and turbulent energy k of fortified wave at 30T and 60T are shown in Fig. 7. Compared the hydrodynamic characteristics at t = 30T with those at t = 60T, it is found that the wave profile and the distribution of velocity are both harmonic at t = 30T. Howevr, the fortified wave is sightly breaking at t = 60T. The distribution of velocity is correspondingly disordered. It also can be observed from the distribution of turbulent energy k that the turbulence at t = 30T is minor. The maximum k is only o.1J at this moment, located at the area far away from the composite breakwater. In front of the breakwater, the turbulent energy k is nearly zero. However, the situation at t = 60T is significantly different. The turbulence becomes considerable at t = 60T. The maximum k reaches up to 1.5J, which is one order greater than that at t = 30T. The turbulence of the fortified wave mainly occurs in the areas near to the free surface and in front of the breakwater. Overall, it seems that the fortified ocean wave tends to become unstable, and breaks with time when interacting with the composite breakwater.

When the fortified ocean wave is simulated, the seabed foundation and rubble mound is treated as porous medium, and the caisson is treated as impermeable rigid object. As a result, there is distribution of water pore pressure in the seabed foundation and rubble mound. However, there is no pore pressure in the caisson. As shown in Fig. 7, the distribution of pore pressure in the seabed foundation and rubble mound is wavy, directly influenced by the ocean waves. Wave-induced dynamic pressure is the driving force causing the seabed foundation response. For example, the pore pressure in the seabed could build up, leading to the softening of seabed soil. As shown in Fig. 7, the distribution of the wave-induced dynamic pressure is periodic. Under the wave crest, the dynamic pressure is positive. Meanwhile, it is negative value under the wave trough. The maximum magnitude of the dynamic pressure acting on the caisson induced by the fortified wave can reach up to about 30 kPa. In the engineering practice, wave-induced force on offshore structures is an important parameter for the stability design of structures. Fortunately, FSSI-CAS 2D can quantitatively predict this wave-induced force applied on offshore structures, as illustrated in Fig. 8. It is demonstrated in Fig. 8 that the amplitude of the dynamics force acting on the caisson induced by the fortified ocean wave is about 800 kN per meter of breakwater. Ocean engineers must make sure that the composite breakwater in the west harbour zone can resist the risk of overturning under this dynamic force.

Another important factor that needs to be considered is the seawater of overtopping. Fig. 9 illustrates the time history of the accumulated volume of seawater (unit: L/m) overtopping the composite breakwater. It is found that the accumulated volume of seawater overtopping per meter breakwater is about 350 L in the period of 90s (time = 155s-245s). The average rate of seawater overtopping is as little as 3.9 L/s m. It is indicated that the composite breakwater at the west harbour zone of Yantai port has adequate abilities to resist the seawater overtopping induced by the fortified ocean wave.

6.2. Dynamics of structure-seabed foundation system

The dynamics of structure and seabed foundation forms the base for evaluation of the stability of offshore structures. In this section, the dynamics of the composite breakwater and its foundation at the west harbour zone of Yantai port is analyzed under the impact of the fortified ocean wave. In the design stage, ocean engineers generally would like to know whether their design structures subside or not, and how much would the structure subside under a fortified ocean wave. For the composite breakwater at the west harbour zone of Yantai port, the computational result illustrated in Fig. 10 can answer the above two questions. The time history of the displacement of the left-top corner of the breakwater clearly indicates that the composite breakwater would subside dramatically, reaching 120 cm after 60T impacted by the fortified ocean wave. At the meantime, the horizontal displacement of composite breakwater reaches 180 cm (to the left side). The dramatical horizontal displacement and subsidence indicate that the composite breakwater at the west harbour zone is gradually tilting to the left side in the impact process of the fortified ocean wave. This tilting process of the composite breakwater is demonstrated in Fig. 11. It can be seen that the composite breakwater is basically stable even through it has subsided 120 cm, and tilts to the left-side 180 cm under the impact of fortified ocean wave.

An interesting phenomenon observed in Fig. 11 is the deformation

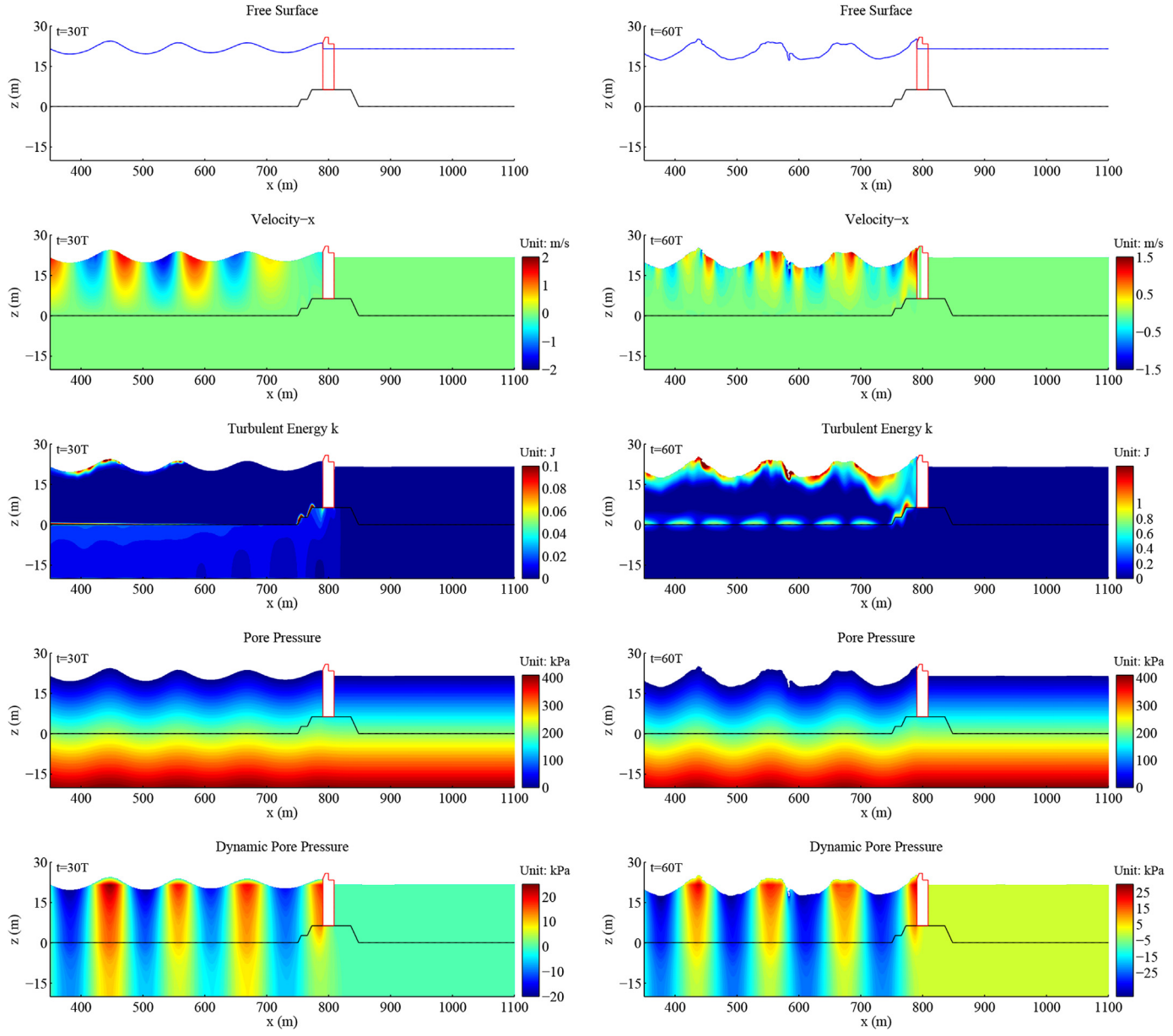

Fig. 7. Wave profile, distribution of pore pressure, dynamic pore pressure, velocity and turbulent energy k at t = 30T and t = 60T

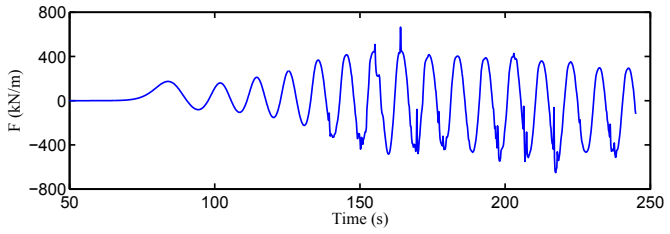

Fig. 8. Fortified ocean wave-induced dynamic force acting on the caisson.

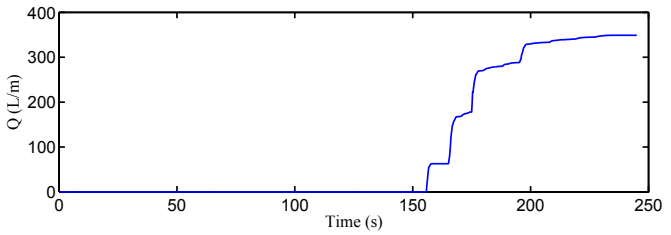

Fig. 9. Accumulated volume of seawater per meter of the breakwater due to wave overtopping.

of the seabed foundation and rubble mound. Due to the fact that the seabed foundation soil at the West Harbour ZOne of Yantai port is relatively loose and has a weak bearing capacity, pore pressure in the seabed foundation will build up under cyclic wave loading, resulting in the softening or liquefaction in the seabed foundation. Exactly because of this reason, the overlaying composite breakwater subsides and tilts to one side, forcing the seabed foundation to deform. As shown in Fig. 11, the seabed soil near to the left part of the rubble mound moves up, simultaneously to the left due to the compression of the settled composite breakwater. Because of the requirement for deformation coordination between the rubble mound and the seabed soil around it, uplift also occurs in the leftmost part of the rubble mound. The magnitude of deformation in the composite breakwater and its seabed foundation is illustrated in Fig. 12. It is clearly seen that the deformation in the foundation zone around the left part of the rubble mound is

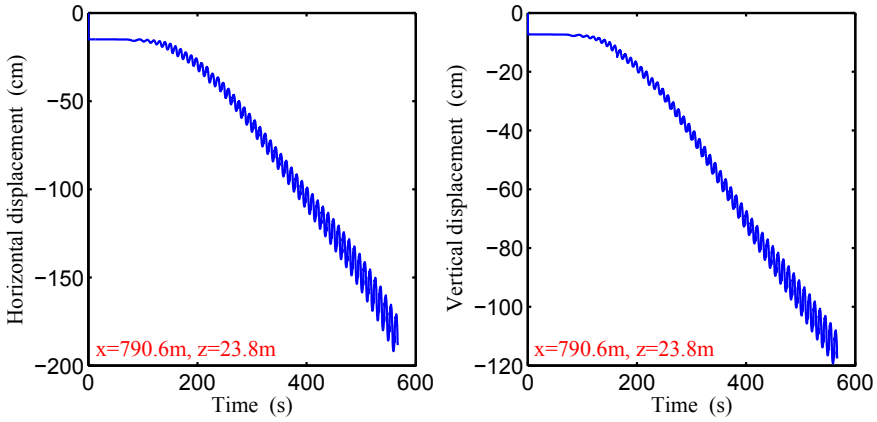

Fig. 10. Displacement of the left-top corner of composite breakwater (x = 790.6 m, z = 23.8 m).

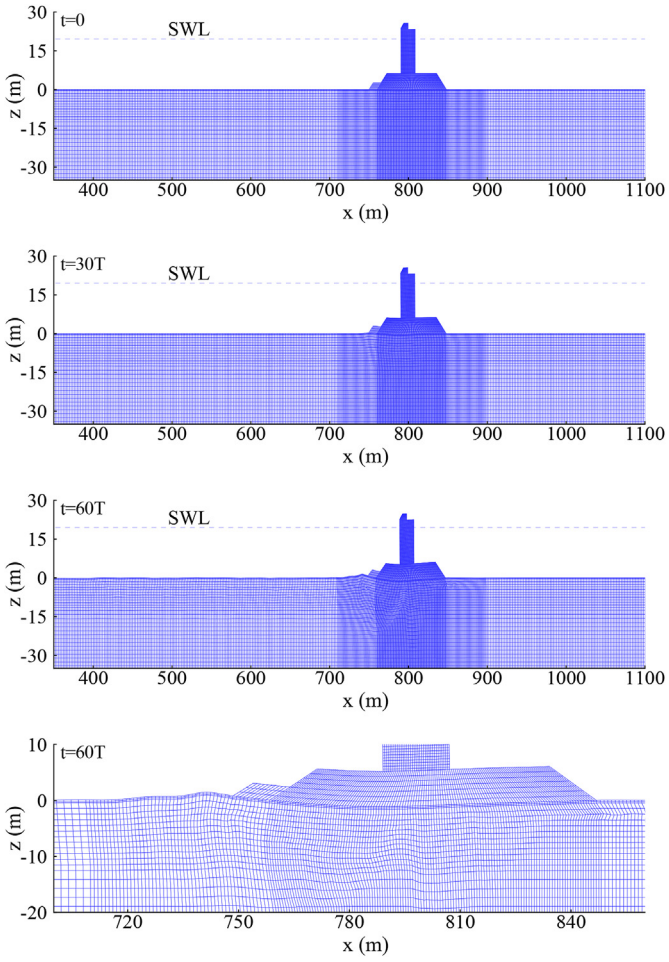

Fig. 11. Deformation process of breakwater-seabed foundation system under fortified ocean wave loading.

most significant. The maximum magnitude of the uplift displacement of the seabed soil in this zone is up to 100 cm.

Except for the deformation, variation of pore pressure and effective stresses in the seabed foundation are also important characteristics of the dynamics. To illustrate this, two typical positions in the seabed foundation are chosen as representative. They are position A (x = 650 m, z = −2.5 m) far away from the composite breakwater, and position C (x = 800 m, z = −2.5 m) under the left part of rubble mound, as shown in Fig. 5. The time histories of pore pressure and effective stresses at the two typical positions A and C are shown in Fig. 13 and Fig. 14. In Fig. 13, it can be seen that pore pressure at position A builds up under the impact of the fortified wave. Correspondingly, the effective stress σ_x' and σ_x' reduce from their initial values 15 kPa and 22 kPa, resulting in the softening of the seabed foundation. To the time t = 350s, σ_z' becomes about 1 kPa, which means that the current stress, between soil particles at position A is less than 5% of its initial value. More than 95% of contact stress between soil particles has vanished. At this moment, the seabed soil at position A can be treated as liquefied soil. Correspondingly, the shear stress at position A basically becomes nearly zero at this moment, because the liquefied soil behaves like a heavy fluid, losing the ability to resist shear stress. As illustrated in Fig. 13, the variation of the effective stresses induced by the fortified ocean wave is complicated. It is shown that the magnitude of the effective stresses σ_x' and σ_z', as well as the amplitude of shear stress τ_{xz} at position A, increase gradually with the impact of the fortified ocean wave after the seabed soil has become liquefied. This phenomenon can not be explained from a linear perspective, and precisely reflects the nonlinear characteristics for the interaction between the wave and the seabed foundation.

In Fig. 14, it can be seen that the characteristic of the dynamic response to the fortified ocean wave at position C under the composite breakwater is significantly different with that at position A. It can be clearly observed that the residual pore pressure at position C dramatically builds up from 225 kPa to 395 kPa before t = 310s, and then it quickly reduces into a range of 350–360 kPa. This reduction process of the pore pressure can undoubtedly be attributed to the mechanism of pore pressure dissipation. Actually, the build up and dissipation of pore

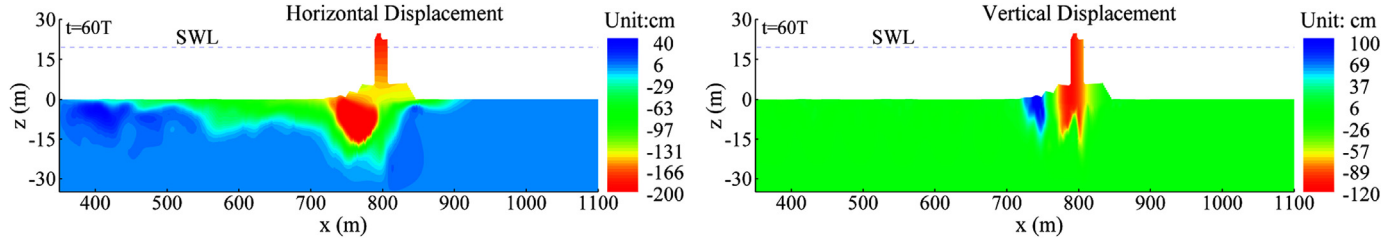

Fig. 12. Distribution of displacement in composite breakwater-seabed foundation at t = 60T

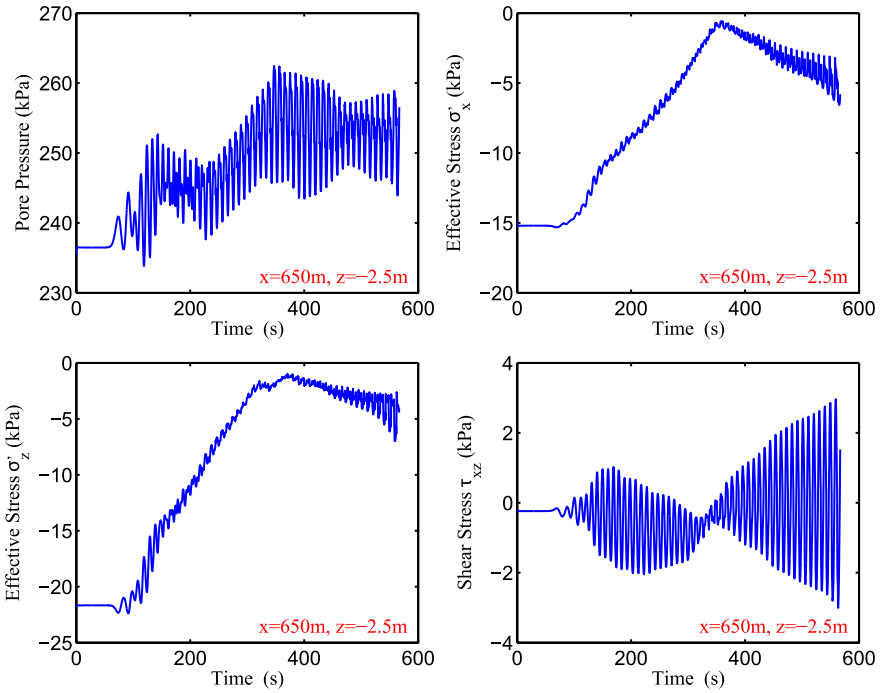

Fig. 13. Pore pressure and effective stresses at position A (x = 650 m, z = −2.5 m) far away from the composite breakwater.

pressure in seabed soil both simultaneously exist. Excess pore pressure occurs in seabed soil exactly due to the fact that the rate of build up of pore pressure is greater than the rate of dissipation. It is also can be seen in Fig. 14 that the effective stresses σ_x', σ_z' and τ_{xz} all increase before t = 210s. However, they all are reduced after t = 210s. Finally, σ_x', σ_z' and τ_{xz} all approach to zero from the time t = 400s, indicating that the seabed soil at position C becomes liquefied at t = 400s.

In Fig. 14, there is an interesting phenomenon to which we need to pay attention. As stated above, the effective stresses at position C all increase before t = 210s. However, the corresponding pore pressure also increases in this period. Furthermore, the pore pressure at position C reduces in the period of t = 310s–400s; while, its effective stresses also reduce in this period. It seems that the classic theory for the effective stress principle in Soil Mechanics is not established in this case. According to the effective stress principle, the effective stresses should reduce in the process of pore pressure build up. Actually, there is a precondition for the above statement that the total stress must be constant. In this study, the effect of the composite breakwater is significant. From the analysis of the displacement of the composite breakwater, it is known that the composite breakwater subsides downward, and tilts to left side under the impact of the fortified ocean wave. In the process of subsiding and tilting, the composite breakwater

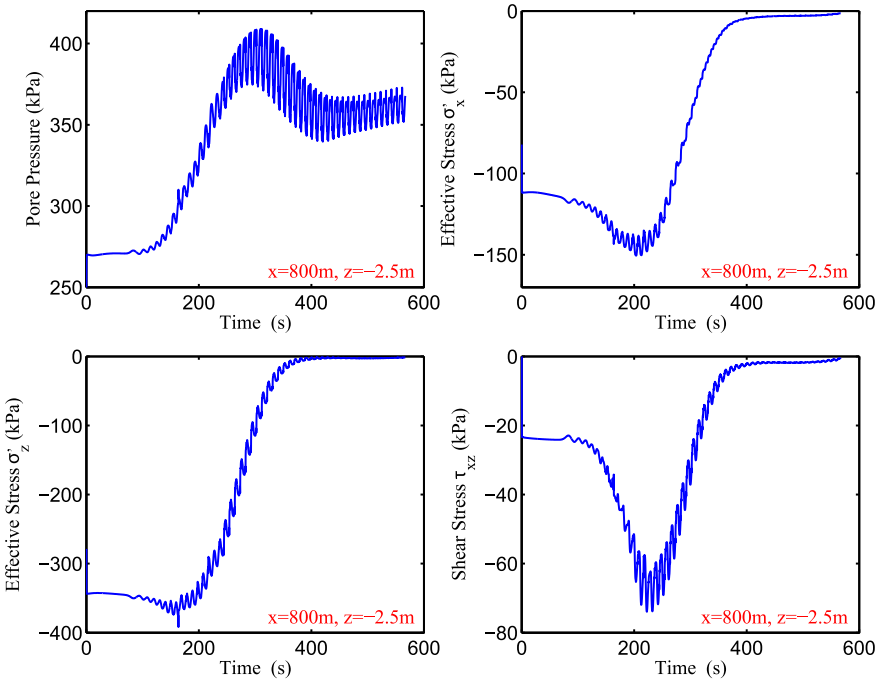

Fig. 14. Pore pressure and effective stresses at position C (x = 800 m, z = −2.5 m) under the composite breakwater.

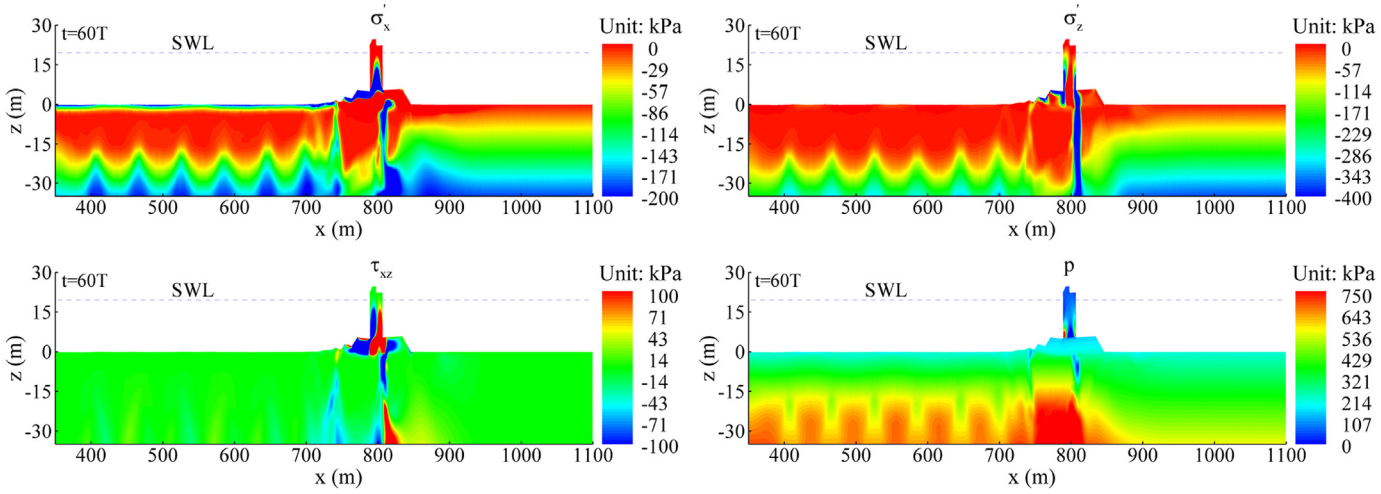

Fig. 15. Distribution of effective stress and pore pressure in composite breakwater-seabed foundation at t = 60T

will apply an additional force on the soil at position C due to the offset of the gravity of the breakwater. As a result, the total stress at position C is not constant. Before t = 210s, the total stress at position C increases, after that it reduces. The complicated variation of the total stress at position C directly leads to the above stated interesting phenomenon demonstrated in Fig. 14. Actually, the classic theory for the effective stress principle in Soil Mechanics is still applicable in this study. From the above analysis, it is known that the interaction between ocean wave, offshore structures and seabed foundation is highly nonlinear. Numerical models are the only ways to handle these kinds of complicated engineering problems.

The above analysis is only based on the computational results at two typical positions in the seabed foundation of the composite breakwater. It is necessary to further study the distribution of wave-induced effective stresses and pore pressure in the seabed foundation. Fig. 15 demonstrates these distributions at t = 60T. It is found that the effect of the fortified ocean wave is mainly concentrated in the seabed at the open sea side. The distribution of σ'_x, σ'_z in the seabed foundation are wavy, obviously significantly affected by the applied wave. In the seabed foundation, the area with red colour where σ'_x, σ'_z approach to zero is huge, indicating that soil liquefaction has occurred in a large area in the seabed foundation, especially in the area under the composite breakwater. Another phenomenon observed in the distribution of pore pressure is that there are a series of core shape areas in which the pore pressure is higher than that in the surrounding zone. It indicates that the build up of pore pressure is not uniform in seabed foundation under ocean wave loading. It also can be seen in the distribution of σ'_z that there is a narrow banded area in which effective stress is huge in the seabed foundation beneath the composite breakwater. This high effective stress banded area behaves like a pile supporting the overlying composite breakwater. Otherwise, the composite breakwater will sink into the liquefied foundation and finally be submerged.

6.3. Liquefaction estimation

It has been widely verified that loose seabed soil can liquefy under ocean wave loading by laboratory tests (Sassa and Sekiguchi, 1999) and field records (Sassa et al., 2006). There are, generally, two types of liquefaction mechanisms for seabed soil. One is momentary liquefaction, only occurring in very dense sand under wave troughs. Its effect on the transient stability of offshore structures is minor. However, momentary liquefaction could boost the scouring of seabed soil around offshore structures. Another is residual liquefaction due to the pore pressure building up in loose soil. The liquefaction occurring in the loose seabed foundation at the west harbour zone of Yantai port in this study is exactly residual liquefaction. Generally, residual liquefaction in seabed foundations has fatal effects on the stability of offshore structures. In this section, the liquefaction is quantitatively estimated for the seabed foundation of composite breakwater at the west harbour zone under fortified ocean wave impacting.

Following Yang and Ye (2017), a parameter being referred to as residual liquefaction potential $L_{potential}$ is defined to quantitatively estimate the liquefaction zone in seabed foundation.

$$L_{potential} = \frac{\sigma'_{zd}}{-\sigma'_{z0} + \alpha c} \tag{19}$$

where $\sigma'_{zd} = \sigma'_z - \sigma'_{z0}$ is wave-induced dynamic vertical effective stress; σ'_{z0} is initial vertical effective stress; σ'_z is current vertical effective stress. c is cohesion of seabed soil; α is a material coefficient. In Equation (19), the cohesion of seabed soil is considered. From the point of view that cohesive soil is much more difficult to become liquefied under cyclic loading, it indicates that soil cohesion could effectively boost the liquefaction resistance of soil $L_r = -\sigma'_{z0} + \alpha c$ (Liu and Jeng, 2016). Therefore, cohesion c of soil must be considered when defining liquefaction potential. Due to the fact that macroscopic cohesion c of soil is not absolutely equivalent to microscopic liquefaction resistance of soil particles, a material coefficient must be added to the cohesion c of soil in Equation (19). Currently, investigations on the effect of cohesion of soil on its liquefaction resistance are limited. In this study, the value of the material coefficient α is set as 0.1. In theory, when $L_{potential}$ is greater than or equal to 1.0, the seabed soil becomes liquefied. According to this definition, $L_{potential}$ is estimated in the seabed foundation of the composite breakwater at the west harbour zone of Yantai port based on the computational results of the effective stresses. The distribution of $L_{potential}$ in the seabed foundation at times t = 10T, t = 20T, t = 40T and t = 60T are illustrated in Fig. 16. The zone with red colour where $L_{potential} \geq 1.0$ is the predicted liquefaction zone. It can be seen that (1) liquefaction first occurs in the zone near to the surface of the seabed foundation; (2) the liquefaction zone in the seabed foundation gradually enlarges with the impact of the fortified ocean wave; (3) the frontier of the liquefaction zone is wavy, and progressively downward. Up to the time t = 60T, most of the seabed foundation soil beneath the composite breakwater becomes liquefied. However, there is still a non-liquefaction banded area beneath the composite breakwater. As stated above, this non-liquefaction zone, with high effective stress behaves like a pile supporting the overlying composite breakwater. Even though most parts of the seabed foundation at west harbour zone of Yantai port become liquefied at t = 60T under the impact of the fortified ocean wave, the computation results given by the integrated model FSSI-CAS 2D clearly indicate that the composite breakwater at the west harbour

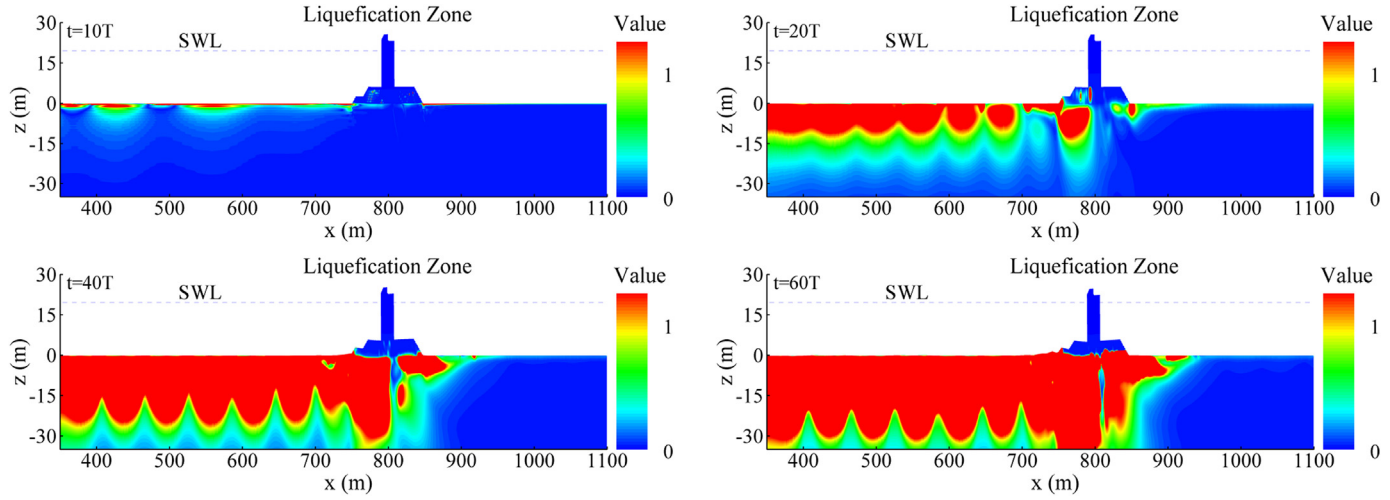

Fig. 16. Liquefaction zone (labelled as red colour) predicted adopting the stress-based criteria. (For interpretation of the references to colour in this figure legend, the reader is referred to the Web version of this article.)

zone only subsides 120 cm, and moves 180 cm to the left. The composite breakwater can still steadily stand on the seabed foundation, indicating that the stability of composite breakwater at the west harbour zone can be guaranteed under the impact of the extreme fortified ocean wave.

Due to the fact that there are terms only related to the effective stress in Equation (19), this criteria is actually a stress-based liquefaction criteria. Except for stress-based criteria, there is another liquefaction criteria based on excess pore pressure, defined as

$$L_p = \frac{p_{excess}}{\sigma'_{z0}} \tag{20}$$

where p_{excess} is the excess pore pressure. This criteria is a pore pressure-based liquefaction criteria. If there is only the seabed floor without a marine structure, then the stress-based liquefaction criteria (Equation (19)) is essentially similar to the pore pressure-based liquefaction criteria (Equation (20)). Because the total stress is kept constant if there is no effect of marine structure, the value of excess pore pressure should be equal to the wave-induced dynamic effective stress according to effective stress principle. However, the difference between the stress-based criteria and the pore pressure-based criteria is considerable if there are marine structures on the seabed foundation, because the total stress is no longer a constant in such cases. According to the definition of soil liquefaction that the effective stress vanishes between soil particles, the stress-based criteria is a direct criteria to estimate the occurrence of soil liquefaction, regardless of whether there are marine structures or not. In the practice of computation, seabed soil can be treated as liquefied soil so long as the current effective stress between soil particles approach to zero. Correspondingly, the pore pressure-based criteria is an indirect criteria. Due to the fact the development of excess pore pressure is complicated in nonlinear cases, where marine structures are involved, it is relatively difficult to link the magnitude of excess pore pressure to soil liquefaction. In other words, there is no absolute connection between excess pore pressure and soil liquefaction. In the cases involving marine structures, seabed soil can not become liquefied even the excess pore pressure has exceeded the initial effective stress. Therefore, the pore pressure-based liquefaction criteria is not reliable in cases marine structures are involved. This unreliability of the pore pressure-based liquefaction criteria is illustrated, taking the seabed foundation at the west harbour zone of Yantai port as a example.

Fig. 17 illustrates the time history of σ'_z, p_{excess} and $L_p = p_{excess}/\sigma'_{z0}$ at position C in the seabed foundation of the composite breakwater at the west harbour zone. It can be seen that the effective stress σ'_z becomes zero from time t = 400s, indicating that the seabed soil at position C is

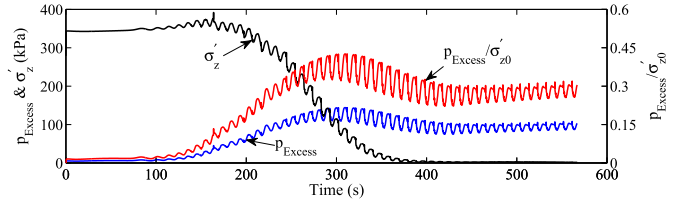

Fig. 17. Time history of vertical effective stress, Excess pore pressure, and $L_p = p_{excess}/\sigma'_{z0}$ at position C (x = 800 m, z = −2.5 m).

liquefied after t = 400s because the effective stress between soil particles has completely vanished. However, the excess pore pressure at position C is only about 100 kPa; and $L_p = p_{excess}/\sigma'_{z0}$ based on the pore pressure-based criteria is only around 0.3 after t = 400s. Therefore, the seabed soil at position C is estimated to be non-liquefied after t = 400s according to the pore pressure-based criteria. This result is of course contradictory to the real situation, where the seabed soil has become liquefied.

The distribution of $L_p = p_{excess}/\sigma'_{z0}$ based on the pore pressure-based criteria in the seabed foundation at t = 30T and 60T are further shown in Fig. 18. Compared with the predicted liquefaction zone (adopting the stress-based criteria) shown in Fig. 16, it is found that the predicted liquefaction zone adopting pore pressure-based criteria is disordered, and significantly different to that shown in Fig. 16. It indicates that the pore pressure-based criteria to estimate liquefaction zone is unreliable in cases where marine structures are involved. It is highly recommended to adopt the stress-based criteria to judge the occurrence of seabed soil liquefaction in the engineering practice.

7. Conclusions

In this study, dynamic response characteristics of the composite breakwater and its seabed foundation at the west harbour zone of Yantai port under the impact of an extreme fortified ocean wave are comprehensively investigated, using the integrated numerical model FSSI-CAS-2D as the computation tool. Based on the computational results, the stability of the composite breakwater at the west harbour zone of Yantai port is further evaluated. This study provides ocean engineers with a demonstration case for the application of integrated model FSSI-CAS 2D in practice. Finally, the following outcomes are obtained from this application case:

(1) The rate of seawater per meter overtopping over the composite

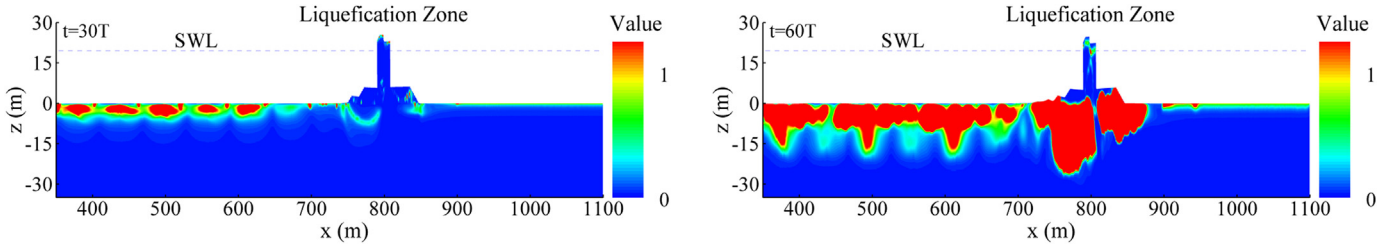

Fig. 18. Liquefaction zone (labelled as red colour) predicted adopting the pore pressure-based criteria. (For interpretation of the references to colour in this figure legend, the reader is referred to the Web version of this article.)

breakwater is as little as 3.9 L/s · m. It indicates that the composite breakwater at the west harbour zone of Yantai port has adequate abilities to resist seawater overtopping induced by the fortified ocean wave.

(2) The amplitude of the wave-induced horizontal impact force acting on the caisson lateral side is 800 kN per meter of breakwater.

(3) Liquefaction can occur in most parts of the seabed foundation on the open sea side under the long-term impact of the fortified ocean wave. This factor would be fatal for the stability of the composite breakwater at the west harbour zone of Yantai port. However, the computation results also confirm that the composite breakwater subsides 1.2 m, and moves 1.8 m to the left side at t = 60T. For such a large scale composite breakwater, this is only slight tilting. Unacceptable subsidence and tilting do not occur for the composite breakwater at the west harbour zone of Yantai port under the impact of the extreme fortified ocean wave. Summarily, the stability of the composite breakwater at the west harbour zone of Yantai port could be guaranteed for a long term service period.

(4) The case study demonstrates that the integrated model FSSI-CAS-2D is proved to be applicable in the practice of complicated engineering. And this integrated model also can be utilized to optimize the design of offshore structures in the future.

Acknowledgements

Professor Jianhong Ye is grateful to the funding support from Strategic Priority Research Program of the Chinese Academy of Sciences, China, Grant No. XDA13010202; and National Natural Science Foundation of China, China, Grant No. 51879257 as well as No. 41472291.

References

Gatmiri, B., 1990. A simplified finite element analysis of wave-induced effective stress and pore pressures in permeable sea beds. Geotechnique 40 (1), 15–30.
Hsu, J.R., Jeng, D.S., 1994. Wave-induced soil response in an unsaturated anisotropic seabed of finite thickness. Int. J. Numer. Anal. Meth. GeoMech. 18 (11), 785–807.
Hsu, T.J., Sakakiyama, T., Liu, P.L.F., 2002. A numerical model for wave motions and turbulence flows in front of a composite breakwater. Coast Eng. 46, 25–50.
Jeng, D.S., Hsu, J.R.C., 1996. Wave-induced soil response in a nearly saturated seabed of finite thickness. Geotechnique 46 (3), 427–440.
Jeng, D.S., Lin, Y.S., 1996. Finite element modelling for water waves-seabed interaction. Soil Dynam. Earthq. Eng. 15 (5), 283–300.
Liao, C.C., Jeng, D.S., Zhang, L.L., 2015. An analytical approximation for dynamic soil response of a porous seabed due to combined wave and current loading. J. Coast Res. 31 (5), 1120–1128.
Liu, B., Jeng, D.S., 2016. Laboratory study for influence of clay content (cc) on wave-induced liquefaction in marine sediments. Mar. Georesour. Geotechnol. 34 (3), 280–292.
Lu, H.B., 2005. The Research on Pore Water Pressure Response to Waves in Sandy Seabed. Master's thesis. Changsha University of Science & Technology, Changsha, Hunan China.
Luan, M.T., Wang, D., 2001. Numerical analyses of dynamic response of porous seabed under wave loading. Chin. Ocean Eng. 19 (4), 40–45.
Madsen, O.S., 1978. Wave-induced pore pressure and effective stresses in a porous bed. Geotechnique 28 (4), 377–393.
Mase, H., Sakai, T., Sakamoto, M., 1994. Wave-induced porewater pressure and effective stresses around breakwater. Ocean. Eng. 21 (4), 361–379.
Mizutani, N., Mostafa, A.M., Iwata, K., 1999. Numerical modeling of nonlinear interaction between wave and composite breakwater over sand bed. J. Hydraul., Coast. Environ. Eng., JSCE 614 (II-14), 121–133.
Mizutani, N., Mostarfa, A., Iwata, K., 1998. Nonliear regular wave, submerged breakwater and seabed dynamic interaction. Coast Eng. 33, 177–202.
Mostafa, A., Mizutani, N., Iwata, K., 1999. Nonlinear wave, composite breakwater, and seabed dynamic interaction. J. Waterw. Port, Coast. Ocean Eng., ASCE 25 (2), 88–97.
Pastor, M., Zienkiewicz, O.C., Chan, A.H.C., 1990. Generalized plasticity and the modelling of soil behaviour. Int. J. Numer. Anal. Meth. GeoMech. 14, 151–190.
Sassa, S., Sekiguchi, H., 1999. Wave-induced liquefaction of beds of sand in a centrifuge. Geotechnique 49 (5), 621–638.
Sassa, S., Takayama, T., Mizutani, M., Tsujio, D., 2006. Field observations of the build-up and dissipation of residual porewater pressures in seabed sands under the passage of stormwaves. J. Coast Res. 39, 410–414.
Shen, J.H., Wu, H.C., Zhang, Y.T., 2017. Subsidence estimation of breakwater built on loosely deposited sandy seabed foundation: elastic model or elasto-plastic model. Int. J. Nav. Architect. Ocean. Eng. 9 (4), 418–428.
Teh, T.C., Palmer, A.C., Damgaard, J.S., 2003. Experimental study of marine pipelines on unstable and liquefied seabed. Coast Eng. 50 (1–2), 1–17.
Tsai, C.P., Lee, T.L., 1995. Standing wave induced pore pressure in a porous seabed. Ocean. Eng. 22 (6), 505–517.
Yamamoto, T., Koning, H., Sellmeijer, H., Hijum, E.V., 1978. On the response of a poro-elastic bed to water waves. J. Fluid Mech. 87 (1), 193–206.
Yang, G., Ye, J.H., 2017. Wave and current-induced progressive liquefaction in loosely deposited seabed. Ocean. Eng. 142, 303–314.
Yang, G., Ye, J.H., 2018. Nonlinear standing wave-induced liquefaction in loosely deposited seabed. Bull. Eng. Geol. Environ. 77 (1), 205–223.
Ye, J.H., 2012. Numerical Analysis of Wave-seabed-breakwater Interactions. PhD thesis. Universtity of Dundee, Dundee, UK.
Ye, J.H., Jeng, D.-S., 2012. Response of porous seabed to nature loadings-waves and currents. J. Eng. Mech., ASCE 138 (6), 601–613.
Ye, J.H., Jeng, D.-S., Liu, P.L.-F., Chan, A.H.C., Wang, R., Zhu, C.-Q., 2014. Breaking wave-induced response of composite breakwater and liquefaction of seabed foundation. Coast Eng. 85, 72–86.
Ye, J.H., Jeng, D.-S., Wang, R., Zhu, C.-Q., 2013a. Numerical study of the stability of breakwater built on sloped porous seabed under tsunami loading. Appl. Math. Model. 37, 9575–9590.
Ye, J.H., Jeng, D.-S., Wang, R., Zhu, C.-Q., 2013b. Validation of a 2D semi-coupled numerical model for Fluid-Structures-Seabed Interaction. J. Fluid Struct. 42, 333–357.
Ye, J.H., Jeng, D.-S., Wang, R., Zhu, C.-Q., 2015. Numerical simulation of wave-induced dynamic response of poro-elasto -plastic seabed foundation and composite breakwater. Appl. Math. Model. 39, 322–347.
Zhou, Y.H., Lu, H.B., Chen, Z.J., 2005. Numerical simulation of pore water pressure response of elastic seabed under wave loading. J. Waterw. Harb., ASCE 26 (2), 67–70.
Zienkiewicz, O.C., Chan, A.H.C., Pastor, M., Schrefler, B.A., Shiomi, T., 1999. Computational Geomechanics with Special Reference to Earthquake Engineering. John Wiley and Sons, England.
Zienkiewicz, O.C., Chang, C.T., Bettess, P., 1980. Drained, undrained, consolidating and dynamic behaviour assumptions in soils. Geotechnique 30 (4), 385–395.